Empirical Modeling of Ducting Effects on a Mobile Microwave Link Over a Sea Surface

Yee Hui LEE[1], *Yu Song MENG*[2]

[1]School of Electrical and Electronic Engineering, Nanyang Technological University
50 Nanyang Avenue, Singapore 639798, Singapore
[2]National Metrology Centre, A*STAR (Agency for Science, Technology and Research)
1 Science Park Drive, Singapore 118221, Singapore

eyhlee@ntu.edu.sg, ysmeng@ieee.org or meng_yusong@nmc.a-star.edu.sg

Abstract. *In this paper, signal enhancement due to the ducts over a sea surface is experimentally investigated and modeled. The investigation is carried out through the study of air-to-ground mobile microwave links over a tropical ocean with low airborne altitudes (0.37 – 1.83 km) at C band (5.7 GHz). The distance-dependence of the ducting induced enhancement (with reference to the free-space propagation) is linearly modeled, and the physical variations of the ducts are found to be Gaussian distributed. Empirical ducting coefficients and parameters for the Gaussian function are estimated and provided for the prediction of the distance-dependent signal enhancement due to the ducts in similar scenarios.*

Keywords

Air-to-ground, channel modeling, ducting, microwave link, propagation.

1. Introduction

In order to achieve a successful implementation of modern wireless systems with high performance, understanding of radio-wave propagations in different media is important [1], [2]. For applications with a slant propagation path such as satellite communications, buildings [3] or trees [4], [5] could cause shadowing along the propagation channel, and therefore degrade the quality of service (QoS). Even for a line-of-sight (LoS) link, specular reflection [6] or ducting [7] can affect the propagating signal of interest. Therefore, proper characterization and modeling of a radio-wave propagation channel is essential for the design of modern wireless systems.

Recently, due to the application of a C-band microwave landing system (MLS) in aviation navigation, we investigated air-to-ground radio-wave propagation channels over a tropical ocean. Results from the channel impulse responses in [8] indicated similar observations to those reported in [6]. That is, a 3-ray multipath model, consisting of a LoS path and two reflected paths, provides a good fit to the measured channel responses. For our channels, about 95 % (86 %) of the measured channel responses can be represented by the 3-ray (2-ray) multipath model. However, the possible signal enhancement due to the ducts over the sea surface is not fully investigated for the radio-wave propagations with low airborne altitudes.

From the literature, radio-wave propagation over a sea surface is well recognized to be affected by the ducts. For example, an evaporation duct above the sea surface can result in a substantial increase in the received signal strength at the frequencies above 3 GHz [9]. Results in [10] also reported that an enhancement larger than 10 dB was observed in 48 % of the time along a 27.7-km over-sea path at 5.6 GHz which is close to our transmission frequency of 5.7 GHz. However, the ducting effects for our measurement scenarios: higher altitudes (up to 1.83 km), longer propagation distance (up to 95 km), and mobile transmission which are different from those reported in [9], [10], is less investigated.

Therefore, in this paper, a detailed investigation of the signal enhancement due to the ducts over a tropical ocean is performed. As a continued work of [11], the main objective of this paper is to characterize and model the distance-dependence of the ducting induced enhancement and the physical variations of the ducts over the sea surface. In the following, a brief description of the measurement setup and environment is given in Section 2. In Section 3, analysis and modelings of the signal enhancement due to the ducting effects are reported. Finally, conclusions of this paper are presented in Section 4.

2. Measurement Campaign

2.1 Measurement Setup

The spread spectrum technique *maximal-length pseudo-noise (PN) sequence* was implemented for channel sounding at the transmitter [12]. In our measure-

ments, a 511-bit *PN sequence* was transmitted at a rate of 20 Mchips/s, with binary phase-shift keying modulation. The predefined signal was transmitted by a vector signal generator, and then passed through a high-power amplifier, before being radiated into the channel of interest via a vertically polarized omni-directional blade antenna. This blade antenna was mounted on the head of the aircraft with an effective radiated power of 40 dBm. GPS data was logged continuously during the flight through a GPS receiver installed on the aircraft throughout the measurement, so as to obtain the instantaneous altitude, longitude, latitude, pitch, roll, and yaw coordinates of the moving aircraft.

(a) Antenna **(b)** Data logger

Fig. 1. On-site measurement setups at ground station (receiver site).

At the receiver, two identical directional antennas (e.g. one shown in Fig. 1a) with a beamwidth of 20° azimuth and 25° elevation were used to create a height (5.55 m) and space (6.45 m) diversity receptor [8], [13]. The received signal was amplified and down-converted to a 22 MHz IF signal, and sampled at a rate of 100 Msamples/s using the data logger as shown in Fig. 1b. The total gain of each receiver front-end consisting of an antenna, a low noise amplifier, a mixer and a low pass filter is about 80 dB. All the data recorded was stamped with the GPS time in order to synchronize the measured data with the aircraft location. Descriptions of the channel sounding technique used in the measurements can be found in [12].

2.2 Measurement Environment

Fig. 2. Open space in the coastal area (receiver site).

To eliminate possible shadowing/multipath effects from the surrounding environments, the ground station in this study is located at an open space at a coastal area on the eastern side of Singapore (1°20'07" N, 104°01'16" E) as shown in Fig. 2. The transmitted signal mainly propagates over the sea surface and there is no blockage of the signal. In this paper, radio-wave propagations along a straight flight path as discussed in [8] will be investigated for the airborne altitudes of 0.37, 0.91, and 1.83 km. This is to minimize the possible shadowing effect due to the aircraft maneuvering [13]. During the whole measurement campaign, there was no rain.

3. Signal Enhancement due to the Ducting Effect

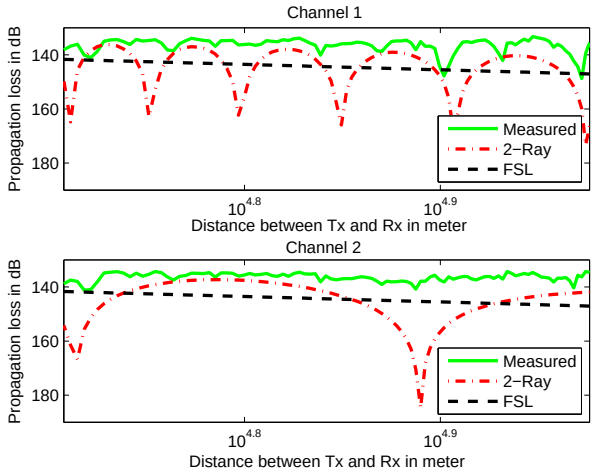

Fig. 3. An example of the propagation loss at the airborne altitude of 1.83 km.

Our previous study [8] shows that the measured path loss is much less than the predicted loss from the free space loss (FSL) model and the 2-Ray loss model [1] for an air-to-ground LoS propagation channel over a tropical ocean at 5.7 GHz. Fig. 3 shows an example of the measured loss at the airborne altitude of 1.83 km against the predicted values from the FSL model and the 2-Ray model. Here, Channel 1 is for the receiver with a height of 7.65 m, and Channel 2 is for the receiver with a height of 2.10 m. Details of the measured propagation loss at other airborne altitudes can be found in [8].

3.1 Spatial Dependence of the Enhancements

In this study, in order to investigate the possible ducting effects, the measured propagation loss is normalized to the predicted values using the FSL model to estimate the measured signal enhancement $P_{enhance-meas}$ in dB. Example of the measured signal enhancement due to the possible ducting effects are shown in Fig. 4 which corresponds to the results for both channels in Fig. 3. From Fig. 4, it is found that, the signal enhancement in dB increases slightly as the transmission distance d increases. This is because a higher portion

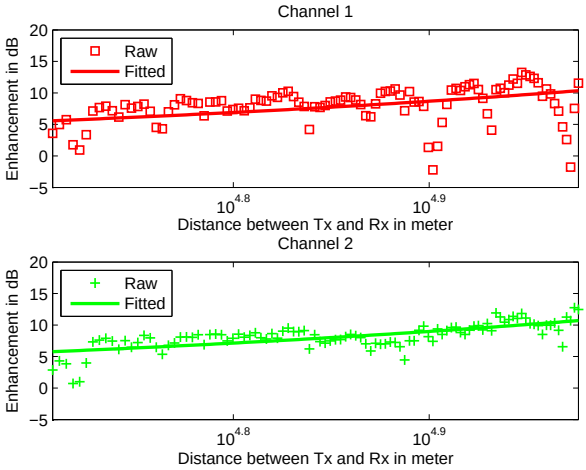

Fig. 4. Spatial variation of the signal enhancement in dB due to the ducting effects at the airborne altitude of 1.83 km.

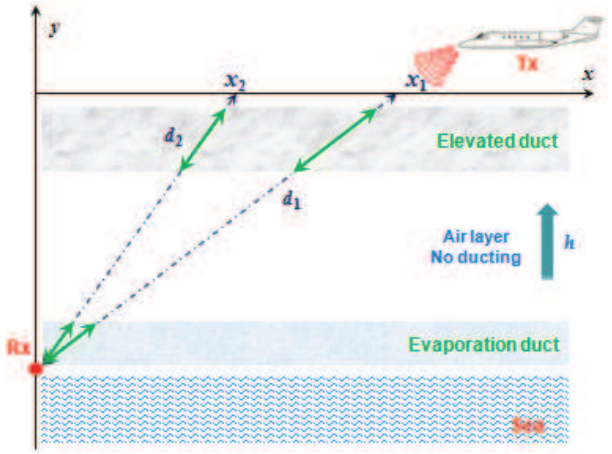

Fig. 5. Simple description of the two possible ducting layers.

of the propagating path traverses the ducting layers and then gets influenced a bit more when d increases (e.g. slightly longer ducted path as highlighted in green when $d_1 > d_2$ as shown in Fig. 5). Moreover, it is noted that there are some deep nulls in the estimated signal enhancement in Fig. 4. The degradation may be due to the specular sea-surface reflections as reported in [8].

Moreover, our previous study [11] reported a simple analysis of the spatial distribution of the signal enhancements in dB which was found to be Gaussian distributed. However, the reported information in [11] is distance-dependent which may not be useful for other transmission scenarios with similar altitudes. Therefore, in this paper, detailed investigations of the distance-dependent ducting effects and their variations are presented.

In this work, with the assumptions of homogenous ducting layers and no enhancement at $d = 0$, the distance dependance of the ideal signal enhancement P_{ducted} is linearly modeled as

$$P_{ducted}(dB) = A * d(km) \quad (1)$$

where A is the resultant ducting coefficient in dB/km where the propagation space (combining the ducting and air layers) is treated as a uniform medium, and d is the transmission distance in km. Here, the reason for treating the whole space as an uniform medium is because; it is quite difficult to identify the boundary of each duct layer and therefore the true length of the ducted path (highlighted in green as shown in Fig. 5) practically. Through the linear regression on the measured data (Examples of regression are shown in Fig. 4), the empirical values for the resultant ducting coefficient A under different flight scenarios are estimated and summarized in Tab. 1.

Flight Scenarios		
$h_{transmitter}$	$h_{receiver}$	A in dB/km
1.83 km	7.65 m	0.1093
1.83 km	2.10 m	0.1131
0.91 km	7.65 m	0.0868
0.91 km	2.10 m	0.1039
0.37 km	7.65 m	0.1110
0.37 km	2.10 m	0.1162
Average		0.1067
Standard Deviation		0.0106

Tab. 1. Empirical values for the resultant ducting coefficient A.

From Tab. 1, it is found that, for all the scenarios, Channel 2 ($h_{receiver} = 2.10$ m) has a consistently higher resultant ducting coefficient A as compared to Channel 1 ($h_{receiver} = 7.65$ m). Since all other conditions are kept the same for both channels during the measurements, the higher resultant ducting coefficient A for Channel 2 compared to those for Channel 1 is due to the difference in the receiver height. The receiver with a lower antenna height has a higher probability to be located within the evaporation duct (adjacent to the sea surface) as shown in Fig. 5.

Moreover, as the airborne altitude increases from 0.37 km to 0.91 km, the resultant ducting coefficient A decreases for both the Channel 1 and Channel 2. This is because the grazing angle increases as the airborne altitude increases, and therefore the transmitted signal from the airborne platform become difficult to be trapped into the evaporation duct.

When the airborne altitude further increases to 1.83 km, the propagating signal is further enhanced (higher resultant ducting coefficient A for both channels) as compared to the results at 0.91 km. This is possibly due to the influence from the elevated duct in the troposphere as shown in Fig. 5. ITU-R P.453 [7] presents the statistics of the atmospheric ducts derived from 20-year radiosonde observations from 1977 to 1996 from 661 sites. The information shows that in our measurement region, the probability of yearly occurrence of the elevated duct is more than 10 % of the time and the average yearly elevated duct height is more than 1 km. Moreover, on-site radiosonde data was also collected near the receiver location in our study. Although the measured radiosonde data has a poor vertical resolution, it indicates the existence of an elevated duct with a height of around 0.9 km to 1 km which

is close to the value obtained from ITU-R P.453 [7]. Therefore, for the air-to-ground radio-wave transmission at an airborne altitude of 1.83 km, besides the evaporation duct, the elevated duct in the troposphere is another important form of ducts which can enhance the air-to-ground over-sea radio-wave propagations, and results in a higher resultant ducting coefficient A as compared to the results at 0.91 km. The observations are consistent with those reported in our previous studies [8], [11].

Furthermore, it is found that although there is a slight difference among the estimated resultant ducting coefficients under different flight scenarios, the values as shown in Table. 1 are close to each other with an average of 0.1067 and a standard deviation of 0.0106. As it is difficult to find the true heights of the ducts in practical applications, the average resultant ducting coefficient of 0.1067 could be a good choice for the rough estimation of the distance-dependent signal enhancement due to the ducts in similar scenarios.

3.2 Statistical Modeling of the Duct Variations

The variations of the measured signal enhancement $P_{enhance-meas}$ have been analyzed using the cumulative distribution function (CDF) for our transmission scenarios [11]. The corresponding empirical CDF distribution for the results at the airborne altitude of 1.83 km in Fig. 4 is shown in Fig. 6. Similar results are observed for the other two airborne altitudes. From Fig. 6, it is found that for both channels, the measured signal enhancement $P_{enhance-meas}$ can be more than 8 dB for 50 % of the propagations.

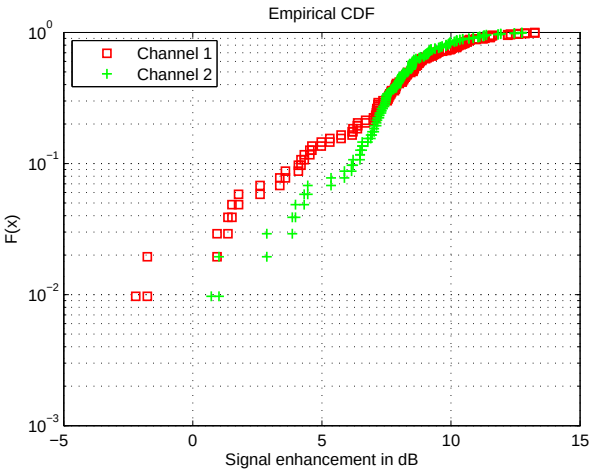

Fig. 6. Empirical CDF distribution for the measured signal enhancement in dB at the airborne altitude of 1.83 km.

However, the distance-dependance of the signal enhancement is not removed for the results in Fig. 6. The displayed results may not show the true response for the physical variations of the ducting layers over the sea surface. Therefore, in this study, investigation of the variations of distance-offset signal enhancement (indicating the physical variations of the ducting layers indirectly) is performed. The influence from the distance is minimized using the derived $P_{ducted}(dB) = A * d(km)$ and shown below,

$$P_{dist-offset}(dB) = P_{enhance-meas}(dB) - A * d(km). \quad (2)$$

The empirical CDF distribution for the processed results using (2) is shown in Fig. 7 for the airborne altitude of 1.83 km with the removal of distance effect. From Fig. 7, it is clearly observed that the CDF curve for Channel 1 is flatter than that for Channel 2. Similar observations are observed for the other two flight altitudes. This indicates there are more physical variations of the ducting layers for Channel 1. This is because the receiver with a higher antenna height (Channel 1 with $h_{receiver}$ of 7.65 m) has a lower probability to be located within the evaporation duct (adjacent to the sea surface) as explained above, and may be located near the boundary of the evaporation duct.

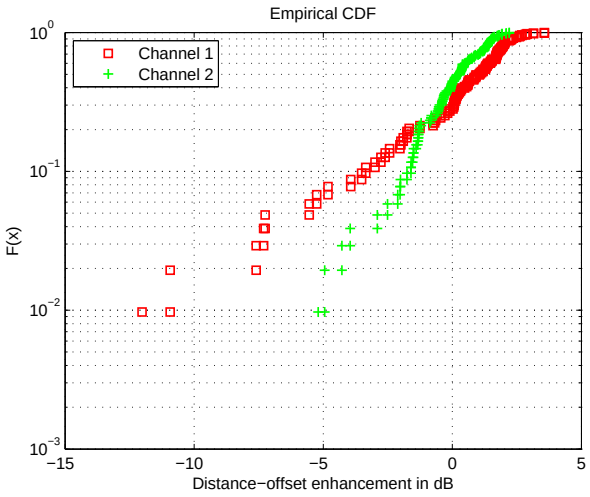

Fig. 7. Empirical CDF distribution for the distance-offset signal enhancement in dB at the airborne altitude of 1.83 km.

In order to characterize the physical variations of the ducting layers, statistical modeling of the distance-offset signal enhancement $P_{dist-offset}$ is performed using three commonly known distributions associated with radio-wave propagation, namely Gaussian, Rician, and Rayleigh as in [1], [2]. The mathematical expressions for each distribution are shown in the following equations.

Gaussian distribution,

$$P_r(r) = \frac{1}{\sigma\sqrt{2\pi}} e^{\frac{-(r-\mu)^2}{2\sigma^2}} \quad (3)$$

where μ and σ are the mean and standard deviation of the random variable r.

Rician distribution,

$$P_r(r) = \frac{r}{\sigma^2} e^{\frac{-(r^2+s^2)}{2\sigma^2}} I_0\left(\frac{sr}{\sigma^2}\right) \quad (4)$$

where $I_0(\bullet)$ is the modified Bessel function of the first kind with zeroth order. In this study, s is the amplitude of the

Flight Scenarios		Distributions		
$h_{transmitter}$	$h_{receiver}$	Gaussian E_{rms}	Rician E_{rms}	Rayleigh E_{rms}
1.83 km	7.65 m	0.1081	0.1082	0.2033
1.83 km	2.10 m	0.0483	0.0483	0.1544
0.91 km	7.65 m	0.1108	0.1115	0.1810
0.91 km	2.10 m	0.0477	0.0477	0.1411
0.37 km	7.65 m	0.0635	0.0635	0.1227
0.37 km	2.10 m	0.0847	0.0848	0.1464

Tab. 2. E_{rms} values for each distribution under different scenarios.

mean signal enhancement in dB, and σ^2 is the variance due to the random variation of the ducting layers.

Rayleigh distribution,

$$P_r(r) = \frac{r}{\sigma^2} e^{\frac{-r^2}{2\sigma^2}} \tag{5}$$

where σ is the standard deviation of the random variation of the ducting layers.

The distribution of the measured data (distance-offset signal enhancement) is compared with the above-mentioned three theoretical distributions with $P_r = P_{dist-offset}$. Using the maximum-likelihood estimation (MLE) method, the theoretical parameters for the three distributions are estimated [14]. The set of parameters that maximizes the likelihood function to fit the measured data is determined. To verify how well the distribution of the measured data fits with the theoretical models using the MLE method, the root-mean-square (RMS) error E_{rms} between the experimental and theoretical distributions is calculated by [14]

$$E_{rms} = \sqrt{\frac{\sum_{i=1}^{N}(E_i^2)}{N}} \tag{6}$$

where N is the number of data points, and E_i is the difference between the experimental and theoretical values at the same fade level. In this test, E_{rms} for each distribution under different flight scenarios are calculated and tabulated in Tab. 2. The theoretical model with the smallest E_{rms} is considered to be the best distribution function of the three for describing the physical variations of the ducts over the sea surface.

From Tab. 2, Gaussian distribution function is found to be the best model of the three for the description of the physical variations of the ducts in general. An example of the best fitted probability density function (pdf) with the experimental distribution at 1.83 km is plotted in Fig. 8. The empirical values for μ and σ of the best fitted Gaussian function for the distance-offset signal enhancement $P_{dist-offset}$ under different flight scenarios are estimated using the MLE method and summarized in Tab. 3.

From Tab. 3, it can be found that Channel 1 with $h_{receiver}$ of 7.65 m has a higher σ which indicates more physical variations of the ducting layers as compared to Channel 2 with $h_{receiver}$ of 2.10 m. This is because the receiver with a higher antenna height has a lower probability to be located within the evaporation duct, and may be located near the boundary of the evaporation duct as explained above.

Flight Scenarios		Gaussian Function	
$h_{transmitter}$	$h_{receiver}$	μ	σ
1.83 km	7.65 m	0.0939	2.7998
1.83 km	2.10 m	0.0005	1.4746
0.91 km	7.65 m	0.2722	5.1077
0.91 km	2.10 m	0.1400	1.4426
0.37 km	7.65 m	0.2249	3.0316
0.37 km	2.10 m	0.2143	2.2244

Tab. 3. Empirical values for μ and σ of the Gaussian function.

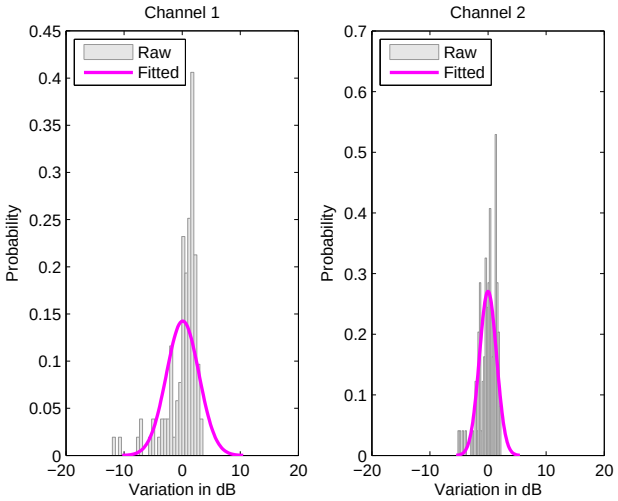

Fig. 8. Best fitted PDF with the experimental distribution for the estimated distance-offset signal enhancement at the airborne altitude of 1.83 km.

4. Conclusions

In this paper, we have reported an experimental investigation of the signal enhancement due to the ducts over a sea surface. The investigation is carried out through the study of air-to-ground radio-wave propagations over a tropical ocean with low airborne altitudes (0.37 – 1.83 km) at C band (5.7 GHz).

In this study, the distance-dependence of the ducting induced enhancement in dB is linearly modeled, and the physical variations of the ducting layers are found to be Gaussian distributed. The estimated resultant ducting coefficients A and the empirical values for μ and σ of the Gaussian function for $P_{dist-offset}$ under different flight scenarios could be used to predict the distance-dependent signal enhancement $P_{enhance-pred}$ due to the ducting effects in similar application scenarios using (7),

$$P_{enhance-pred}(dB) = A * d(km) + P_{dist-offset}(dB). \tag{7}$$

Moreover, study in [15] reported the influence of the sea surface roughness on the radio-wave propagations in the duct environment, and found that the roughness can be intensified with the increase in the sea-wind speed. However, due to the limitations of experimental condition in this study, the information on instantaneous sea-wind speed is lacking, and therefore, further investigations are needed.

Acknowledgements

This work was supported in part by the Defence Science and Technology Agency, Singapore.

References

[1] PARSONS, J. D. *The Mobile Radio Propagation Channel,* 2nd ed. Chichester (UK): Wiley, 2000.

[2] BERTONI, H. L. *Radio Propagation for Modern Wireless Systems,* 1st ed. Upper Saddle River (NJ, USA): Prentice Hall, 2000.

[3] SIMUNEK, M., PECHAC, P., FONTAN, F. P. Excess loss model for low elevation links in urban areas for UAVs. *Radioengineering*, 2011, vol. 20, no. 3, p. 561 - 568.

[4] MENG, Y. S., LEE, Y. H. Investigations of foliage effect on modern wireless communication systems: A review. *Progress In Electromagnetics Research*, 2010, vol. 105, p. 313 - 332.

[5] HORAK, P., PECHAC, P. Excess loss for high elevation angle links shadowed by a single tree: measurements and modeling. *IEEE Transactions on Antennas and Propagation*, 2012, vol. 60, no. 7, p. 3541 - 3545.

[6] LEI, Q., RICE M. Multipath channel model for over-water aeronautical telemetry. *IEEE Transactions on Aerospace and Electronic Systems*, 2009, vol. 45, no. 2, p. 735 - 742.

[7] ITU-R P.453-10. *The Radio Refractive Index: Its Formula and Refractivity Data.* Geneva (Switzerland): International Telecommunication Union, 2012.

[8] MENG, Y. S., LEE, Y. H. Measurements and characterizations of air-to-ground channel over sea surface at C-band with low airborne altitudes. *IEEE Transactions on Vehicular Technology*, 2011, vol. 60, no. 4, p. 1943 - 1948.

[9] HITNEY, H. V., HITNEY, L. R. Frequency diversity effects of evaporation duct propagation. *IEEE Transactions on Antennas and Propagation*, 1990, vol. 38, no. 10, p. 1694 - 1700.

[10] HEEMSKERK, H. J. M., BOEKEMA, R. B. The influence of evaporation duct on the propagation of electromagnetic waves low above the sea surface at 3-94 GHz. In *Proceedings of the Eighth International Conference on Antennas and Propagation.* Edinburgh (UK), 1993, p. 348 - 351.

[11] LEE, Y. H., MENG, Y. S. Analysis of ducting effects on air-to-ground propagation channel over sea surface at C-Band. In *Proceedings of the 2011 Asia-Pacific Microwave Conference.* Melbourne (Australia), 2011, p. 1678 - 1681.

[12] LEE, Y. H., MENG, Y. S. Evaluation of laboratory equipments as channel sounding system for mobile radio propagation. In *Proceedings of the 2012 IEEE International Symposium on Antennas and Propagation and USNC-URSI National Radio Science Meeting.* Chicago (USA), 2012.

[13] MENG, Y. S., LEE, Y. H. Study of shadowing effect by aircraft maneuvering for air-to-ground communication. *AEU - International Journal of Electronics and Communications*, 2012, vol. 66, no. 1, p. 7 - 11.

[14] MENG, Y. S., LEE, Y. H., NG, B. C. The effects of tropical weather on radio-wave propagation over foliage channel. *IEEE Transactions on Vehicular Technology*, 2009, vol. 58, no. 8, p. 4023 - 4030.

[15] ZHAO, X., HUANG, S. Influence of sea surface roughness on the electromagnetic wave propagation in the duct environment. *Radioengineering*, 2010, vol. 19, no. 4, p. 601 - 605.

About Authors ...

Yee Hui LEE received the B.Eng. (Hons.) and M.Eng. degrees in electrical and electronics engineering from the Nanyang Technological University, Singapore, in 1996 and 1998, respectively, and the Ph.D. degree from the University of York, York, U.K., in 2002. Since July 2002, she has been with the School of Electrical and Electronic Engineering, Nanyang Technological University where she is currently an Associate Professor. Her interest is in channel characterization, rain propagation, antenna design, electromagnetic bandgap structures, and evolutionary techniques.

Yu Song MENG received the B.Eng. (Hons.) and Ph.D. degrees in electrical and electronic engineering from Nanyang Technological University, Singapore, in June 2005 and February 2010, respectively. From May 2008 to June 2009, he was a research engineer with the School of Electrical and Electronic Engineering, Nanyang Technological University, Singapore. From July 2009 to August 2011, he was a research fellow, and then a scientist with the Institute for Infocomm Research, A*STAR (Agency for Science, Technology and Research), Singapore. In September 2011, he was transferred to the National Metrology Centre, A*STAR, Singapore, where he is currently a scientist. His research interests are in the fields of the developments of national microwave measurement standards and calibration systems, and the study of radio-wave propagations in different media.